

Citation for published version: Le, CD & Kolaczkowski, ST 2015, 'Steam gasification of a refuse derived char: reactivity and kinetics', Chemical Engineering Research & Design, vol. 102, pp. 389-398. https://doi.org/10.1016/j.cherd.2015.07.004

DOI:

10.1016/j.cherd.2015.07.004

Publication date: 2015

Document Version Peer reviewed version

Link to publication

Publisher Rights CC BY-NC-ND

University of Bath

Alternative formats

If you require this document in an alternative format, please contact: openaccess@bath.ac.uk

General rights

Copyright and moral rights for the publications made accessible in the public portal are retained by the authors and/or other copyright owners and it is a condition of accessing publications that users recognise and abide by the legal requirements associated with these rights.

If you believe that this document breaches copyright please contact us providing details, and we will remove access to the work immediately and investigate your claim.

Download date: 09. Mar. 2023

Open Access

This near final version of the paper has been made available by the University of Bath, so that individuals who are unable to access the published final version, can at least read this near final version of the paper which describes the research work that was completed.

However, you **must** take note of the following:

- Errors & Omissions: As this version is a near final draft, it may still contain errors and omissions. You are strongly advised to read the final published version of this paper (although that may even still contain errors).
- **Copyright:** This early version of the paper is protected by copyright, however, that copyright has most probably been transferred or assigned to the publishing company who produced the final version of the paper.
- **Liability:** Neither the authors, nor the University of Bath, accept any liability from the use of information or procedures which may be described in this paper.

Professor Stan Kolaczkowski 10 Dec 2015

Department of Chemical Engineering

University of Bath, Bath, UK

1	Steam gasification of a refuse derived char: Reactivity and kinetics
2	
3	C. D. Le ^{a, b,*} , S. T. Kolaczkowski ^b
4	^a Department of Oil Refining and Petrochemistry, Hanoi University of Mining and
5	Geology, Duc Thang, Bac Tu Liem, Hanoi, Vietnam
6	^b Department of Chemical Engineering, University of Bath, Bath, BA2 7AY, UK
7	
8	Abstract
9	A char was obtained from a commercial pilot-scale gasifier, which had been operating
0	with a refuse derived fuel (RDF). Using this char, steam gasification experiments were
1	then performed in a 15.6 mm i.d. packed bed tubular reactor. The effect of reaction
2	temperature was studied (800 °C to 900 °C), and also the partial pressure of steam were
3	in the range 33.3 kPa to 66.7 kPa. With the aid of the Shrinking-Core and the Uniform-
4	Reaction models, kinetic parameters were estimated (apparent activation energy varied
5	from 96 kJ mol ⁻¹ to 162 kJ mol ⁻¹). It was also found that at lower carbon conversions
6	(e.g. 10 % to 60 %) the RDF-derived char appeared to be more reactive than other bio-
7	chars reported in the literature. However, at higher conversions (> 60 %), its apparent
8	reactivity decreased with carbon conversion, thereby behaving in a similar manner to
9	chars derived from coal.
0	
1	Key words: Kinetic, steam gasification, RDF-derived char, biomass.
2	
3	

1. Introduction

There is much interest in the development of processes in which biomass (e.g. wood) and refuse derived fuels (RDFs) may be converted into a gaseous stream, which could then be used as a fuel to produce energy, or act as a chemical intermediate. Based on information in the literature, it is well recognized that when biomass is gasified in the presence of air, then a gas mixture of CO, H₂, CO₂, N₂ and H₂O is produced, and a char stream is also produced as a by-product [1, 2, 3, 4]. In such processes, the char arises from the nature of the gasification process, where some of the carbon in the feedstock remains, combined with the residual ash, which needs to be removed from the process. As such biomass gasification processes are being developed, there has been great interest in the conversion of the residual carbon in the char into a gaseous fuel, and such a process could be developed using steam to gasify the char.

1.1. Motivation for the gasification of RDF derived char

In their discussions with a number of different companies that were developing such biomass to energy processes, the authors of this paper were made aware of the importance that such companies placed on the need to find economically viable ways of

List of Abbreviations

AAEM Alkali and Alkaline Earth Metallic

QMS Quadrupole Mass Spectrometer

RDF Refuse Derived Fuel

TGA Thermo Gravimetric Apparatus

converting the carbon in the char into a useful form of gaseous fuel. Otherwise, the char produced had to be disposed of off-site, which created a disposal cost and a loss in revenue from the potential of converting the carbon in the char into gaseous fuel. These considerations led to the work described in this study. In such processes, there is thermal energy available, which could be used to produce steam on-site. So using steam in such a process makes sense.

Although there have been many kinetic studies performed on the steam gasification of char [5, 6, 7], these in general have been performed on char from wood, food waste, and coal. There is relatively little data on the gasification of char produced from a process using a refuse derived fuel (RDF). However, it is well recognized that char reactivity depends not only on operating parameters (e.g. temperature, pressure, steam ratio), but also on the source of the char and how it was produced. For example, wood char reactivity is reported to increase with carbon conversion [8], whereas that of coal char decreases with carbon conversion [9]. The presence of inorganic elements in the char may also have a favourable catalytic effect, e.g. [1]

1.2. Effect of temperature

Many of the studies in the literature on the steam gasification kinetics of chars are performed at temperatures in the region of 700 °C to 1000 °C, reflecting the temperature range inside the reaction zone of a gasifier (fluidized/fixed bed), for example, in:

Paviet *et al*. [10] - char gasification experiments are performed with steam at 850 °C, 900 °C, 950 °C and 1000 °C.

67	Khor et al. [11] - charcoal gasification experiments are performed with steam and
68	air at 800 °C to 950 °C in the bed.
69	Chaudhari et al. [3] - steam gasification of chars at 700 °C, 750 °C, and 800 °C.
70	According to Blasi [12], at such high temperatures (<1000 °C), the rate of diffusion
71	through the pores of reacting chars plays no role in determining the overall rate of
72	reaction, so measurements at such high temperatures are considered to be in the
73	kinetically controlled regime. In some of the studies reported in the literature, by
74	making comparisons between the time-scales of the different phenomena involved, a
75	simplified approach to kinetic analysis has been adopted. Such a technique is described
76	in Dupont et al. [13], who applied it to a study on the gasification of biomass with
77	steam.
78	Particle size will also have an effect, and this is discussed in Section 1.4.
79	
80	1.3. Effect of gas velocity
81	
82	The effect of gas velocity was also considered in some studies. For example,
83	Paviet et al. [5] reported that gas velocity had influence on the external mass transfer
84	resistance, and at high gas velocity (from 10 cm s ⁻¹ to 20 cm s ⁻¹) this influence could be
85	considered to be negligible. Mermoud et al. [8] also suggested that gas velocity had a
86	gentle influence on gasification.
87	
88	1.4. Effect of particle size
89	

Char particle size was reported to have no effect by some authors (e.g. Paviet et
al. [5]), while others (e.g. Mermoud et al. [8]; Mani et al. [14]) have reported that as the
particle size is increased, then this has a retarding effect on the rate.

Paviet *et al.* [5], in an investigation of the effects of diffusional resistance on wood char gasification in a tubular kiln reactor, reported no significant influence on wood char gasification for mean char particle sizes of 0.1 mm and 0.47 mm. They suggested that internal mass transfer effects at these conditions could be considered to be negligible (experiments at T = 900 °C to 1000 °C, and steam partial pressure from 10.1 kPa to 70.9 kPa).

Mani *et al*. [13], in an investigation of reaction kinetics and mass transfer of wheat straw char with CO_2 using a thermo gravimetric apparatus (TGA), found that particle size (from less than 60 μ m to 925 μ m) had much influence on the char gasification reaction, and reactivity decreased as the particle size increased (experiments performed at T = 750 °C to 900 °C, with CO_2 partial pressure of 101 kPa).

Mermoud *et al*. [8] formed similar conclusions as Mani *et al*. [14]. However, they investigated the steam gasification of single wood charcoal particles (10 mm to 30 mm in size) at different temperatures (830 °C to 1030 °C), and at different steam partial pressures (10.1 kPa to 40.5 kPa). They concluded that internal mass transfer was influencing the reaction under these operating conditions – although this is not surprising as the charcoal particles were relatively large.

1.5. Effect of alkali and alkaline metallic (AAEM) species

It is well-known that AAEM species can act as good catalysts for the combustion and gasification of solid carbonaceous fuels such as biomass or biochar [1, 15]. As reported in Yip *et al.* [15], during char gasification, the reactivity of the raw biochars generally increased, while that of all acid-treated biochars (for removal of AAEM species) remained relatively unchanged with conversion. The results indicate that Na, K, and Ca retained in the biochars were the key catalytic species, with the catalytic effect appearing to be in the order K > Na > Ca during the steam gasification of the biochar.

A similar phenomenon of increased reactivity of biochar with conversion was also observed and reported by Wu *et al.* [1]. The catalytic effect of the inherent AAEM species seems in turn to depend on the carbon structure that probably affects the catalyst dispersion. It was emphasized that the surface area of biochar increased with conversion, suggesting the formation of new pores and/or opening of closed pores as a result of steam activation during gasification. Besides the effect of the carbon structure evolution, the inhibiting effect of some inorganic components such as Si and P was also discovered by Hugnon et al. [16], where K would tend to be encapsulated by P and Si with carbon conversion, and would then be unable to act as a catalyst.

Nevertheless, consideration of the effects of catalysts and evolution of carbon structure during gasification will not be considered in any detail in this paper; however, they will be used to explain the evolution of reactivity of RDF-derived char during the gasification process.

1.6. Decisions taken

Based on this review, it was decided that the influence of: char particle size, gas flow, char bed length, reaction temperature and steam partial pressure should all be explored. This would lead to the development of useful kinetic rate expressions, which in the future could be used to help estimate the residence time required in a reactor to achieve the desired conversion of carbon in the char. This work is clearly novel, as there is relatively little information in the literature on the gasification kinetics of RDF-derived char.

derived char.

In developing the experimental technique, a number of important assumptions were made based on the following:

- (a) In the literature, it has been suggested (e.g. Everson *et al*. [17] and Huang *et al*. [18]) that char-CO₂ and char-H₂O reactions proceed on separate active sites at atmospheric pressure. Thus, in this present study, it was decided to study the steam (H₂O) gasification of char as a set of experiments on their own.
- (b) Although some authors (e.g. Everson *et al.* [17]; Huang *et al.* [18]) have presented evidence of the inhibition effects of CO in CO₂-char reactions, and H₂ in steam-char reactions, in this study it is assumed that there are no inhibition effects.
- (c) The partial pressure of the gasifying agent (H₂O) is considered to remain unchanged along the reactor, even though it is inevitably consumed in reality.
 This assumption was also applied in other studies in the literature (e.g. Wu et al. [7]; Yip et al. [15]).
- (d) Many of the kinetic experiments on char gasification have been performed using a TGA, and the carbon conversion was measured by the loss in the weight of the sample [8, 14, 17, 18, 19]. However, in this study, it was decided to perform

such experiments in a small packed-bed reactor, which is often used in heterogeneous catalytic experiments. A fast gas analysis method developed in [20] using a quadrupole mass spectrometer (QMS) was used to measure the product gas composition on-line, which was then used to calculate the rate of carbon conversion in the char.

2. Experimental Procedure

2.1. Experimental Apparatus

The experimental work was carried out using a packed-bed reactor (Figure 1), which operated at atmospheric pressure. The reactor consisted of a vertical stainless steel tube with an inner diameter of 15.6 mm, which was filled with RDF-derived char particles. The char bed depth could be varied from 1.6 mm to 23.7 mm. This tube was positioned inside an electrically heated furnace, and the temperature inside the char bed was measured using a thermocouple located at the top of the char bed. The char bed was supported by two quartz wool layers which retained the char and ash particles.

In experiments with steam, the water and nitrogen passed through a stainless steel tube put inside the furnace, which vaporized the water and preheated the gas. The nitrogen flow was adjusted with a rotameter, while that of the water was set using a metering pump.

The gas exiting from the top of the reactor flowed through a cooling coil, and condensate was trapped in two plastic vessels (connected in series). The gas then passed through a glass wool filter, and was finally discharged into the vent from the fume

cupboard. A gas sample stream was passed to a quadrupole mass spectrometer (QMS) for on-line gas analysis.

Figure 1 here

2.2. RDF-derived Char Particle Size Distribution

- Sieves were used to classify by size the RDF-derived char that had been obtained from the commercial pilot-scale gasifier. Information on the fixed carbon content in the different char size ranges will be also useful when designing a process.
- The frequency mass fractions were calculated from:

196
$$q_i = \left(\frac{m}{\Delta d_q}\right)_i \quad \text{or} \quad Q_i = \sum_{1}^{i} (q \Delta d_q)_i$$
 (1)

- where: q_i is the differential frequency mass (or fixed carbon content) fraction of size interval i, μm^{-1} ; Q_i is the cumulative frequency mass (or fixed carbon content) fraction of particles smaller than size $(d_q)_i$; $(\Delta d_q)_i$ is the size interval i, μm ; and m_i is the mass fraction of char particle in size interval i.
- Then, the mean size of the RDF-derived char particles was estimated from:

202
$$\bar{d}_{q} = \frac{1}{\sum_{all \ i} (m/d_{q})_{i}} = 305.52 \,\mu\text{m}$$
 (2)

The results of such a char particle distribution are presented, in Figure 2, from which it can be seen that particle size varied from 37.5 μ m to 7,000 μ m. As the mean size of the RDF-derived char was 305 μ m, a sieve was used to obtain a char particle size range of 250 to 500 μ m (representing mean particle size), and this size range was used for the experiments.

Figure 2 here

From the data on the fixed carbon content (Figure 2(c)), it is interesting to note that this changes slightly with particle size, and this is most probably related to the part of the process from which that carbon particle arose (e.g. carried in the gas stream and trapped in a cyclone, or retained in the char stream from the base of the gasifier).

The results of proximate analysis of the RDF-derived char are: moisture 4.59 wt.% wet basis; volatiles 10.71 wt.% dry basis; fixed carbon 34.18 wt.% dry basis; ash 55.10 wt.% dry basis. The proximate analysis of the RDF pellets was also performed, giving: moisture 7 wt.% wet basis; volatiles 43 wt.% dry basis; fixed carbon 31 wt.% dry basis; ash 26 wt.% dry basis.

From these measurements, it was decided to use char in the size range of 250 μm to 500 μm for the kinetic experiments.

2.3. Experimental Methodology

A bucket of RDF-derived char, obtained from an actual gasification pilot-plant that used RDF pellets as fuel, was supplied by Refgas Ltd, Sandycroft. This char was sealed and stored at room temperature, and used throughout this study to ensure the repeatability of the char resource.

Samples of char were first conditioned by heating for 3 hours in a flow of N_2 at 800 °C, and this removed any volatiles (checked with the QMS). Then N_2 was fed into the reactor (during the heating-up period) to achieve the desired operating temperature.

- 232 This was then followed by the addition of water which turned into steam, and the
- 233 experiment was started. The system pressure was atmospheric (open end of reactor).
- 234 After each run, air was passed through the reactor to burn out any residual carbon.
- Finally, the reactor was cooled, and the remaining ash was collected and weighed.
- The rate of carbon conversion in the char can be inferred from the molar flow
- rate of CO and CO₂ from the reactor. This approach has been used in many studies [5, 6,
- 7, 9, 10], making use of the flow of an inert sweeping gas (e.g. N₂ or Argon) to perform
- such calculations. If the formation of CH₄ was significant then it would have to be
- included, but this was checked and found not to be the case in the experiments
- described.
- The experimental conversion of carbon in the char, X, may be defined (e.g. in
- 243 Paviet *et al.*[5]) as:

$$X = \frac{w_0 - w}{w_0 - w_{ash}} \tag{3}$$

- 245 where: w_0 is the initial sample weight, w is the sample weight at any time t and w_{ash} is
- the ash content measured after reaction.
- The evolution of sample weight, w(t), as a function of time is unknown, but it
- can be deduced from the gas composition. The experimental kinetic rate, at any time t,
- can thus be calculated (e.g. in Cozzani [19]) from:

$$\frac{dX}{dt} = \lim_{\Delta t \to 0} \left(\frac{X_{t_2} - X_{t_1}}{\Delta t} \right) \tag{4a}$$

- where: X_{t_1} and X_{t_2} are carbon conversion at time t_1 and t_2 , respectively; and
- $\Delta t = t_2 t_1 \approx 20 \, s$, which is the measurement step of the gas analysis method.
- 253 or (e.g. in Paviet *et al*. [5]) from:

 $\frac{dX}{dt} = \frac{12(F_{CO} + F_{CO_2})}{w_0 - w_{ash}}$ 254 (4b) where: F_{CO_2} and F_{CO_2} are molar flow rates (mol/min) of CO and CO₂, respectively, in 255 256 the gas stream from the packed bed. 257 Both Equations (4a) and (4b) were tested, and they produced the same results. 258 Equation (4b) was used in this work. 259 260 3. Results and Discussion 261 262 3.1. Experimental Results 263 To determine the operating conditions for the kinetic study the following set of 264 preliminary experiments was performed: 265 266 3.1.1. Effect of char bed length 267 First of all, some preliminary experiments were performed with different char 268 bed lengths (1.6 mm, 5.7 mm, 8.2 mm, 16.8 mm and 23.7 mm), corresponding to 269 different initial mass quantities of char (0.1 g, 0.35 g, 0.5 g, 1.03 g and 1.45 g). The bulk 270 density of the char is 500 kg m⁻³. Experiments were performed at: furnace temperature set at 900 °C; char particles from 250 µm to 500 µm; N₂ flow set at 0.2 L min⁻¹ (1 L = 1 271 dm³; 1 min = 60 s); H₂O flow set at 0.148 g min⁻¹; and an calculated molar ratio of 272

It was observed that the performance of the reactor with bed lengths from 1.6

mm to 16.8 mm was very similar and about 70 % of the carbon in the char was

273

274

275

 $H_2O:N_2 = 1:1$.

consumed after eight minutes. This means that in such a sample the resistance to external mass transfer is negligible.

For the planned kinetics study, it was decided to select a small initial bed length to reduce any secondary reactions, and to minimize the change in the partial pressure of steam along the char bed. However, if a bed length < 5.7 mm was used, then CO concentration would be low, leading to measurement errors. Therefore, an initial char bed length of 8.2 mm was selected for all subsequent experiments.

3.1.2. Effect of gas flow

Experiments were performed at different gas inlet flows ($N_2 = 0.2 \text{ L min}^{-1}$, 0.4 L min⁻¹, 0.6 L min⁻¹ and 0.7 L min⁻¹; $H_2O = 0.148 \text{ g min}^{-1}$, 0.296 g min⁻¹, 0.444 g min⁻¹ and 0.518 g min⁻¹), which corresponded to different superficial velocities in the packed bed (0.218 m s⁻¹, 0.437 m s⁻¹, 0.655 m s⁻¹ and 0.764 m s⁻¹). The experiments were done at the following conditions: furnace temperature set at 900 °C; char bed length = 8.2 mm; char particles from 250 μ m to 500 μ m; calculated molar ratio of $H_2O:N_2 = 1:1$.

It was observed that at the high gas superficial velocities (0.437 m s⁻¹ to 0.764 m s⁻¹), the gas velocity has little influence on char gasification, indicating that external mass transfer resistance is low. In Paviet *et al*. [5], superficial gas velocities at 10 cm s⁻¹ to 20 cm s⁻¹ (0.1 m s⁻¹ to 0.2 m s⁻¹) had little influence on external mass transfer. Although high gas velocities are preferred, this leads to higher errors in CO measurements in the outlet gas stream; hence, a gas velocity of 0.218 m s⁻¹ was selected for subsequent experiments.

3.1.3. Effect of char particle size

Experiments were performed with char particles that had the following size
ranges: 180 μm to 250 $\mu m;$ 250 μm to 500 $\mu m;$ 1000 μm to 1180 $\mu m;$ and 2000 μm to
4000 μm . The experiments were done at: furnace temperature set at 900 $^{\circ}\text{C}$; char bed
length = 8.2 mm ; N_2 flow set at 0.2 L min^{-1} ; H_2O flow set at 0.148 g min^{-1} ; calculated
molar ratio of $H_2O:N_2 = 1:1$.
The results obtained showed that the rate of carbon conversion increases slightly
as the particle size was reduced. However, the increase was insignificant in the size

range tested. Also, because the measured mean particle size of RDF-derived char was approximately 305 μm, particles in the range of 250 μm to 500 μm were chosen for the subsequent kinetic experiments.

3.1.4. Effect of Reaction Temperature

To explore the effect of reaction temperature, experiments were performed at: 800 °C, 850 °C and 900 °C. This set of experiments (at different reaction temperature) was repeated at various H₂O flows, while N₂ flow was kept constant at 0.2 L min⁻¹. This helps to determine kinetic parameters that will be described later. One example of the conditions in the reactor for one set of experiments was: N_2 flow rate = 0.2 L min⁻¹; char bed length = 8.2 mm; H_2O flow = 0.222 g min^{-1} ; calculated molar ratio of $H_2O:N_2 = 3:2$, corresponding to steam partial pressure of 60 kPa.

As expected, reaction rates increased with temperature, see Figure 3.

Figure 3 here

3.1.5. Effect of Partial Pressure of Steam

324	As a reminder, for each reaction temperature (800 °C, 850 °C, or 900 °C),
325	experiments were performed at different partial pressures of H ₂ O (33.3 kPa, 50 kPa, 60
326	kPa and 66.7 kPa), which corresponded to different H_2O flows (0.074 g min ⁻¹ , 0.148 g
327	min^{-1} , 0.222 g min^{-1} and 0.296 g min^{-1}), while N_2 flow was kept constant at 0.2 L min^{-1} .
328	One example of the conditions in the reactor was: furnace temperature set = $850 {}^{\circ}\text{C}$; N_2
329	flow = $0.2 L \text{ min}^{-1}$; char bed length = 8.2 mm .
330	The results are presented in Figure 4, for experiments performed at 850 °C.
331	From these experiments, char reactivity increases with steam partial pressure.
332	
333	Figure 4 here
334	
335	3.2. Kinetic Analysis
335 336	3.2. Kinetic Analysis
	3.2. Kinetic Analysis There are several well established approaches which can be used to develop a
336	
336 337	There are several well established approaches which can be used to develop a
336337338	There are several well established approaches which can be used to develop a model to describe reacting char. Because the ash content in the RDF-derived char is
336337338339	There are several well established approaches which can be used to develop a model to describe reacting char. Because the ash content in the RDF-derived char is high, then according to Levenspiel [21] and Kunii and Levenspiel [22], then either the
336 337 338 339 340	There are several well established approaches which can be used to develop a model to describe reacting char. Because the ash content in the RDF-derived char is high, then according to Levenspiel [21] and Kunii and Levenspiel [22], then either the Uniform-Reaction Model or the Shrinking-Core Model for porous solids of unchanging
336 337 338 339 340 341	There are several well established approaches which can be used to develop a model to describe reacting char. Because the ash content in the RDF-derived char is high, then according to Levenspiel [21] and Kunii and Levenspiel [22], then either the Uniform-Reaction Model or the Shrinking-Core Model for porous solids of unchanging size could be applied. In general, small particles follow the Uniform-Reaction Model,
336 337 338 339 340 341 342	There are several well established approaches which can be used to develop a model to describe reacting char. Because the ash content in the RDF-derived char is high, then according to Levenspiel [21] and Kunii and Levenspiel [22], then either the Uniform-Reaction Model or the Shrinking-Core Model for porous solids of unchanging size could be applied. In general, small particles follow the Uniform-Reaction Model, while large particles follow the Shrinking-Core Model - with ash diffusion controlling at

3.2.1. Estimate of Kinetic Parameters for the Shrinking-Core Model

The theoretical development of this model is based on Levenspiel [21] and
Kunni and Levenspiel [22]. In summary: for a Shrinking-Core model, the reaction front
advances from the outer surface into the particle, leaving behind a layer of ash. Thus, at
any time there exists an unreacted core of carbon which shrinks in size during the
reaction. The driving force of the gasification is proportional to the available surface
area, and char reactivity of a batch particle can be defined as:

353
$$r = \frac{1}{(1-X)^{2/3}} \frac{dX}{dt} = k \cdot P_{H_2O}^n$$
 (5)

- 354 where: $r = \frac{1}{(1-X)^{2/3}} \frac{dX}{dt}$ is called specific (or apparent) reactivity of char in
- 355 gasification reaction [15].
- A similar equation to Equation (5) can also be seen in the literature (e.g.
- 357 Liliedahl and Sjostrom [23]; Basu [24]).
- For the steam gasification of char, an nth-order reaction model is commonly used
- 359 [6, 24]:

$$360 r = k.P_{H_2O}^n (6)$$

- where: P_{H_2O} is the partial pressure of steam, that is considered as the partial pressure of steam in the inlet gas stream.
- From the experimental data of carbon conversion rate, the values of the rate

 constant k, the reaction order n, apparent activation energy E and pre-exponential factor E A were calculated. Figure 5 shows an example of the plots to determine the values of E and E are very encouraging as the data points are positioned close to the 'best-fit' straight lines.

 Values of E and E and E and E and E are shown in Tables 1 and 2, respectively. From these, the

apparent activation energy varied from 96 to 106 kJ mol⁻¹ across the 10 % to 70 % conversion range, and then it increased dramatically to 152 kJ mol⁻¹ at 80 % carbon conversion.

Figure 5 here

Table 1 here

Table 2 here

Blasi [12] reviewed data on the steam gasification of a number of different biochars, and reported that *E* varied from 143 to 237 kJ mol⁻¹ (with a large part of the values around 180 to 200 kJ mol⁻¹), depending on reaction conditions and biochar source. This indicates that the RDF-derived char used in this study may be very active.

From data in Table 2, the value of the pre-exponential factor increases slightly with conversion across the 10 % to 70 % range, but more rapidly after that. This change may be due to the evolution of the char structure with carbon conversion. Ahmed and Gupta [6] suggested that ash might have increased the adsorption rate of steam to the char surface, leading to an increase in the pre-exponential factor. However, (a) increased porosity, and (b) access to the ash (which may have catalytic and inhibiting properties), may also have a role to play [1, 7]. The effects of carbon structure on char reactivity are also discussed in Aarna and Suuberg [25], where they concluded that the micropores (< 2 nm) probably did not participate in the gasification reaction of chars, and that the surface developed by the macropores and the mesopores (2 nm < diameter < 50 nm) was a better indicator of the reactive surface, than the total pore surface area. This conclusion is consistent with others (e.g. Paviet *et al.* [5]; Mermoud *et al.* [26])

In other studies on the steam gasification of biochars [1, 6, 8, 15, 27] pore surface area and reactivity of chars increased with conversion, while an opposite trend was observed for the steam gasification of coal chars [7, 23, 28].

It was decided, to examine the 70 % to 80 % carbon conversion region in more detail, and more data points were added. Figure 5(c) shows the Arrhenius plot for conversions from 71 % to 80 %. A 'compensation effect' is observed here, where there is a simultaneous increase in apparent activation energy and pre-exponential factor with conversion, see Table 2. This 'compensation effect' or 'isokinetic effect' has been observed and reported in the literature for char-gas reactions [6, 7], and explains the observed change that took place.

3.2.2. Estimate of kinetic parameters for the Uniform-Reaction Model

For the Uniform-Reaction Model, the driving force for the gasification is proportional to the mass of unreacted carbon in the particle, and char reactivity of a batch particle can be defined as:

408
$$r = \frac{1}{1 - X} \frac{dX}{dt} = k P_{H_2O}^n$$
 (7)

A similar equation to Equation (7) can also be seen in the literature [22, 23, 24].

For this model, the values of the apparent activation energies (E) and preexponential factors (A) at different degrees of conversion (X) are calculated and presented in Table 3.

414 Table 3 here

It is interesting to note, that when comparing the values of the apparent activation energy (E) calculated in Table 3 (Uniform-Reaction Model), with the values in Table 2 (Shrinking-Core Model), then very similar results have been obtained. This means, that the two models would produce very similar results across the range of conditions tested. However, values of the pre-exponential factor (A) in the Uniform-Reaction Model are different from those in the Shrinking-Core Model. Mathematically, this comes from the fact that the pre-exponential factor in Shrinking-Core Model includes the factor that is a function of the density of carbon and diameter of the char particles, whereas that in the Uniform-Reaction Model does not (deduced from Kunii and Levenspiel [22]).

3.3. Comparison between RDF-derived char and wood charcoal

Finally, a few experiments were performed using a wood based charcoal, obtained from a small commercial gasification reactor that used wood chips as fuel. A bucket of this char, supplied by Refgas Ltd, Sandycroft, was sealed and stored at room temperature, and used throughout this study to ensure the repeatability of this char resource. Two different ranges of wood charcoal particles were used (250 μ m to 500 μ m and 2000 μ m to 4000 μ m) and tested. All of these experiments were performed at: furnace temperature set at 900 °C; char bed length = 8.2 mm; N₂ flow set at 0.2 L min⁻¹; H₂O flow set at 0.148 g min⁻¹; calculated molar ratio of H₂O:N₂ = 1:1.

Figure 6 here

The results are shown in Figure 6.

From these data, it is clear that at low carbon conversion (< 60 %), the RDF-derived char is much more reactive than wood charcoal. However, at higher carbon conversions the opposite is true.

In some studies [15, 28], the reactivity of gasification of char is presented as the specific (or apparent) reactivity, r. If the Shrinking-Core Model is selected, then

 $r = \frac{1}{(1-X)^{2/3}} \frac{dX}{dt}$. Figure 6(c) shows the evolution of apparent reactivity of char with

447 carbon conversion.

From Figure 6(c), above a carbon conversion of 60 %, the apparent RDF-derived char reactivity decreases sharply with carbon conversion. This behaviour of RDF-derived char is opposite to that of other biochars such as mallee-bimass-derived char [14] or food-waste-derived char [6]; however, it is similar to that of coal char (e.g. as presented in Wu *et al.* [7]; Liu *et al.* [9]; Liliedahl and Sjostrom [22]; Xu *et al.* [27]).

Mermoud *et al.* [8], in a study of steam gasification of single wood charcoal particles (with a diameter of 10 mm to 30 mm), observed that the reactivity of wood charcoal increased continuously with conversion due to a continuous increase in the surface area. However, Liu *et al.* [9] reported a decrease in coal char reactivity with conversion because of a decrease in the surface area.

The RDF-derived char contained 55 wt.% ash, which consisted of inorganic elements. It is well known that these elements can have a catalytic effect, which could be the main reason for the increase in reactivity at low carbon conversion (<60%). However, the presence of inorganic elements can also decrease the porosity to such an extent that the active surface area is also decreased [1, 6, 7, 12]. In addition, Hugnon et al. [16] noticed that during steam gasification of algal and lignocellulosic biomass, K

would tend to be encapsulated by P and Si with carbon conversion, and would then be unable to act as a catalyst. Therefore, from the results obtained in this paper, at higher (>60%) carbon conversion, a higher ash content is expected, which could result in an encapsulation of AAEM species, a decrease in porosity (and active surface area), and hence reactivity.

4. Conclusions

For the steam gasification of the RDF-derived char, the apparent activation energy E varied from 96 kJ mol⁻¹ to 162 kJ mol⁻¹. The reactivity of the char (at carbon conversions from 10 % to 60 %) appears to be higher than other biochars reported in the literature. However, at high conversions (> 60 %), the apparent reactivity of the RDF-derived char decreases with carbon conversion, behaving in a similar manner to coal structures.

Comparisons between the use of the Shrinking-Core Model and the Uniform-Reaction Model produced almost identical results.

Information has been presented in this paper, which provides data on the properties of an RDF-derived char and how it could be gasified in the presence of steam. This supports the viability of converting this type of char into a useful fuel gas, which would enhance the commercial viability of the overall 'RDF to energy' process. Such data on RDF-derived char are scarce in the literature, and this is probably the first detailed kinetic study of its type in which kinetic parameters for an RDF-derived char have been determined. These parameters could be used in modelling studies to explore

487	differe	nt design concepts (e.g. packed-bed, moving-bed, fluidized l	ped) for the 'char-
488	gasifie	r', although they would of course then need to be tested in p	ilot-scale studies.
489			
490	Ackno	wledgment	
491			
492	We are	grateful for the support received from Refgas Ltd a compar	ny developing
493	biomas	ss to energy processes, and also for the support from the Vie	tnam Ministry of
494	Educat	ion & Training, in the form of a research grant for C. D. Le.	
495			
496	Nomei	nclature	
497			
498	A	Pre-exponential factor	bar ⁻ⁿ s ⁻¹
499	d_q	Diameter of char particle	μm
500	\overline{d}_q	Mean char particle diameter	μm
501	$(\Delta d_q)_i$	Char particle size interval <i>i</i>	μm
502	E	Activation energy	kJ mol ⁻¹
503	F_i	Molar flow rate of species i	mol/min
504	k	Specific (or apparent) reaction rate coefficient	bar ⁻ⁿ s ⁻¹
505	m_i	Mass fraction of char particle in size interval i	
506	n	Reaction order	
507	P_{H2O}	Partial pressure of steam	bar(a)
508	q	Differential frequency mass (or fixed carbon content)	
509		distribution of char particle size	μm^{-1}
510	q_i	Differential frequency mass (or fixed carbon	

511		content) fraction of size interval i	μm^{-1}
512	Q	Cumulative frequency mass (or fixed carbon content)	
513		distribution of char particle size	
514	Q_i	cumulative frequency mass fraction of particles smaller	
515		than size $(d_q)_i$	
516	r	Specific (or apparent) reactivity of char in gasification	s ⁻¹
517	R_g	Universal gas constant	8.314 J.mol K ⁻¹
518	t	Time	S
519	Δt	Time interval	S
520	T	Temperature	oC.
521	w	Char sample weight at any reaction time t	g
522	w_0	Initial char sample weight	g
523	Wash	Ash content measured after gasification reaction of char	g
524	X	Carbon conversion at any reaction time t	%
525			
526	Refe	erences	
527	[1]	Wu H, Yip K, Tian F, Xie Z, Li CZ. Evolution of char struct	ture during the steam
528		gasification of biochars produced from the pyrolysis of various	ous mallee biomass
529		components. Ind. Eng. Chem. Res. 2009; 48(23): 10431-104	38.
530	[2]	Knoef HAM, editer. Handbook Biomass Gasification. BTG	biomass technology
531		group; 2005.	
532	[3]	Chaudhari ST, Dalai AK, Bakhshi NN. Production of Hydro	gen and/or Syngas
533		(H ₂ + CO) via steam gasification of biomass-derived chars.	Energy and Fuel 2003;
534		17(4): 1062-1067.	

- 535 [4] Kolaczkowski S, Le CD, Jodlowski P. Gasification of wood pellets in an
- experimental quartz tube gasifier How visual 1D experiments can aid 3D design
- considerations. In Proceedings of the bioten conference on biomass and biofuels
- 538 2010, Bridgwater AV, editor, CPL Press UK; 2011, p. 720-732.
- 539 [5] Paviet F, Bals O, Antonini G. The effects of diffusional resistance on wood char
- gasification. Process Safety and Environment Protection 2008; 86: 131-140.
- 541 [6] Ahmed II, Gupta AK. Pyrolysis and gasification of food waste: Syngas
- characteristics and char gasification kinetics. Applied Energy 2010; 87: 101-108.
- 543 [7] Wu S, Wu J, Li L, Wu Y, Gao J. The reactivity and kinetics of yanzhou coal chars
- from elevated pyrolysis temperatures during gasification in steam at 900-1200°C.
- Trans IchemE, Part B, Process Safety and Environmental Protection 2006; 84(B6):
- 546 420-428.
- 547 [8] Mermoud F, Golfier F, Salvador S, Van de Steene L, Dirion JL. Experimental and
- numerical study of steam gasification of a single charcoal particle. Combustion
- and Flame 2006; 145: 59-79.
- 550 [9] Liu H, Luo C, Kato S, Uemiya S, Kaneko M, Kojima T. Kinetics of CO₂
- gasification at elevated temperatures. Part I: Experimental results. Fuel Processing
- Technology 2006; 87: 775-781.
- 553 [10] Paviet F, Bals O, Antonini G. Kinetic study of various chars steam gasification.
- International Journal of Chemical Reactor Engineering 2007; 5: Article A80.
- 555 [11] Khor A, Ryu C, Yang Y, Sharifi VN, Swithanbank J. Clean Hydrogen Production
- via Novel Steam-Air Gasification of Biomass. WHEC 16/13-16. Lyon France;
- 557 2006.

- 558 [12] Blasi CD. Combustion and gasification rates of lignocellulosic chars. Process in
- Energy and Combustion Science 2009; 35: 121-140.
- 560 [13] Dupont C, Boissonnet G, Seiler JM, Gauthier P, Schweich D. Study about the
- kinetic processes of biomass steam gasification. Fuel 2007; 86: 32-40.
- [14] Mani T, Mahinpey N, Murugan P. Reaction kinetics and mass transfer studies of
- biomass char gasification with CO₂. Chemical Engineering Science 2011; 66: 36-
- 564 41.
- 565 [15] Yip K, Tian F, Hayashi J, Wu H. Effect of alkali and alkaline earth metallic
- species on biochar reactivity and syngas composition during steam gasification.
- 567 Energy Fuels 2010; 24: 173-181.
- 568 [16] Hognon C, Dupont C, Grateau M, Delrue F. Comparison of steam gasification
- reactivity of algal and lignocellulosic biomass: Influence of inorganic elements.
- 570 Bioresource Technology 2014; 164: 347-353.
- 571 [17] Everson RC, Neomagus HWJP, Kasaini H, Njapha D. Reaction kinetics of
- 572 pulverized coal-chars derived from inertinite-rich coal discards: Gasification with
- 573 carbon dioxide and steam. Fuel 2006; 85: 1076-1082.
- 574 [18] Huang Z, Zang J, Zhao Y, Zhang H, Yue G, Suda T, Narukawa M. Kinetic studies
- of char gasification by steam and CO₂ in the presence of H₂ and CO. Fuel
- 576 Processing Technology 2010; 91: 843-847.
- 577 [19] Cozzani V. Reactivity in oxygen and carbon dioxide of char formed in the
- 578 pyrolysis of refuse-derived fuel. Ind. Eng. Chem. Res. 2000; 39: 864-872.
- 579 [20] Le, C.D., Kolaczkowski, S. and McClymont, D.W.J. Using a quadrupole mass
- 580 spectrometer for on-line gas analysis gasification of biomass and refuse derived
- 581 fuel. Fuel. 2015; 139: 337-345.

- 582 [21] Levenspiel O. Chemical Reaction Engineering. 3rd ed. John Wiley & Sons; 1999.
- 583 [22] Kunii D, Levenspiel O. Fluidization Engineering. 2nd ed. Butterworth-
- 584 Heinemann; 1991.
- 585 [23] Liliedahl T, Sjostrom K. Modeling of char-gas reaction kinetics. Fuel 1997; 76(1):
- 586 29-37.
- 587 [24] Basu P. Biomass Gasification and Pyrolysis. Elsevier Inc; 2010.
- 588 [25] Aarna I, Suuberg EM. Change in reactive surface area and porosity during char
- oxidation. Twenty-Seventh Symposium (International) on Combustion/The
- 590 Combustion Institute; 1998, p. 2933-2939.
- 591 [26] Mermoud F, Salvador S, Van de Steene L, Golfier F. Influence of the pyrolysis
- heating rate on the steam gasification rate of large wood char particles. Fuel 2006;
- 593 85: 1473-1482.

- 594 [27] Golfier F, Van de steene L, Salvador S, Mermoud F, Oltean C, Bues MA. Impact
- of peripheral fragmentation on the steam gasification of an isolated wood charcoal
- particle in a diffusion-controlled regime. Fuel 2009; 88: 1498–1503.
- 597 [28] Xu Q, Pang S, Levi T. Reaction kinetics and producer gas compositions of steam
- gasification of coal and biomass blend chars, part 1: Experimental investigation.
- 599 Chemical Engineering Science 2011; 66: 2141-2148.

601	Figure Captions
602	
603	Figure 1. Schematic of the kinetic study apparatus.
604	Figure 2. RDF-derived char particles: (a) differential frequency mass and fixed carbon
605	content distributions, (b) cumulative frequency mass and fixed carbon content
606	distributions, (c) fixed carbon content based on char particle size.
607	Figure 3. Influence of reaction temperature: (a) carbon conversion, (b) rate of carbon
608	conversion.
609	Figure 4. Influence of steam partial pressure at 850 °C: (a) carbon conversion, (b) rate
610	of carbon conversion.
611	Figure 5. Plots to estimate kinetic values: (a) Example of plot to determine the values of
612	k and n at 850 °C (Shrinking-Core Model); (b) Arrhenius plot for conversions from 10
613	to 80 $\%$ (Shrinking-Core Model); (c) Arrhenius plot for conversions from 71 to 80 $\%$
614	(Shrinking-Core Model).
615	Figure 6. Comparisons between RDF-derived char and wood charcoal at 900 °C: (a)
616	carbon conversion, (b) rate of carbon conversion, (c) apparent reactivity.
617	

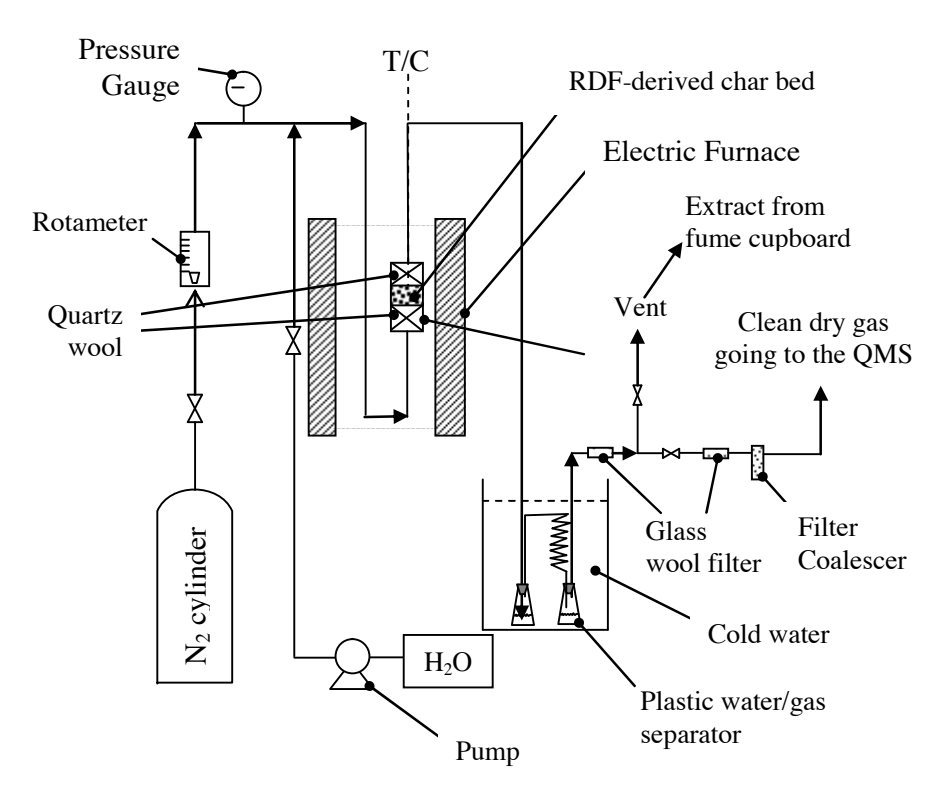


Figure 1

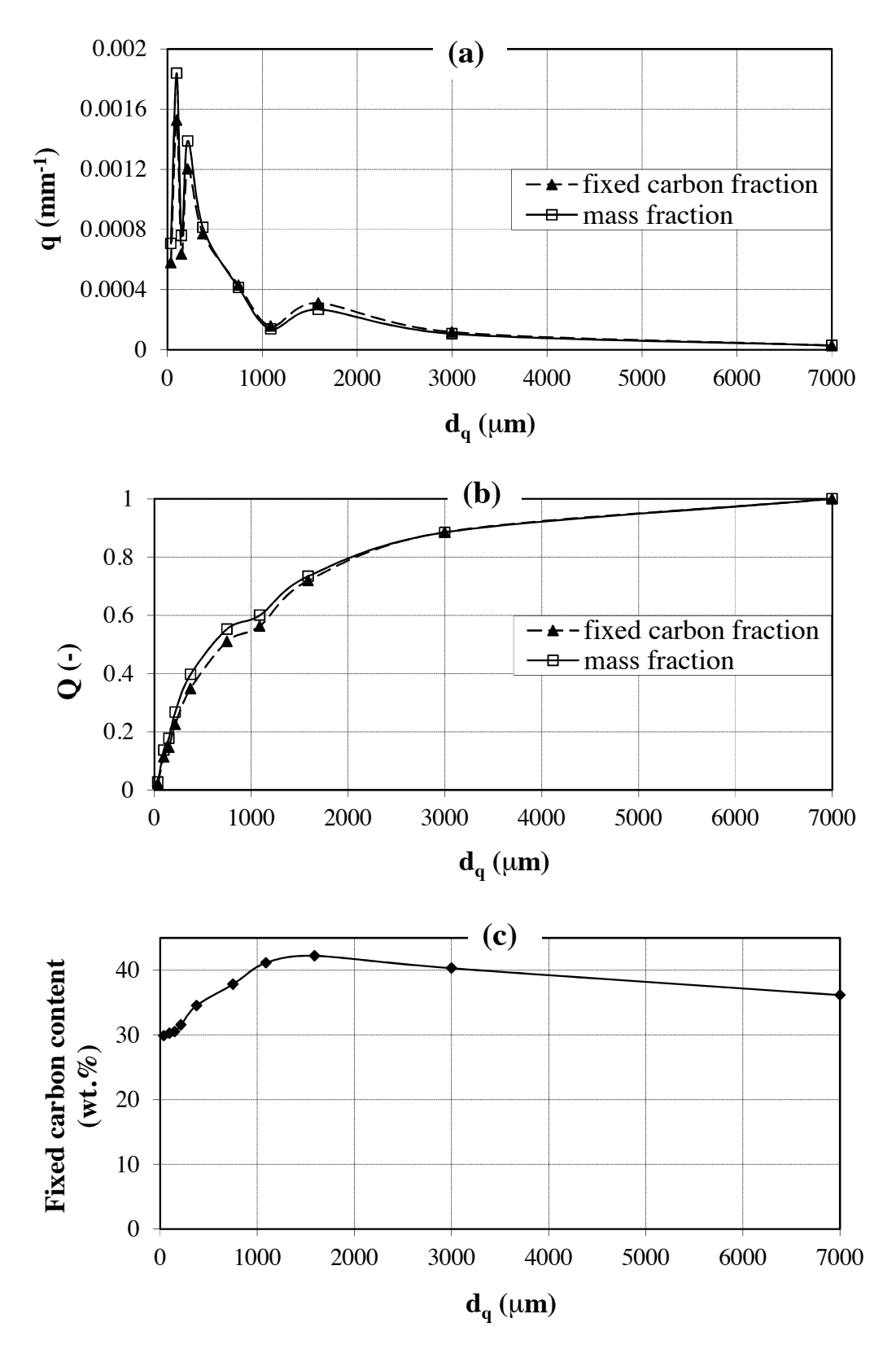
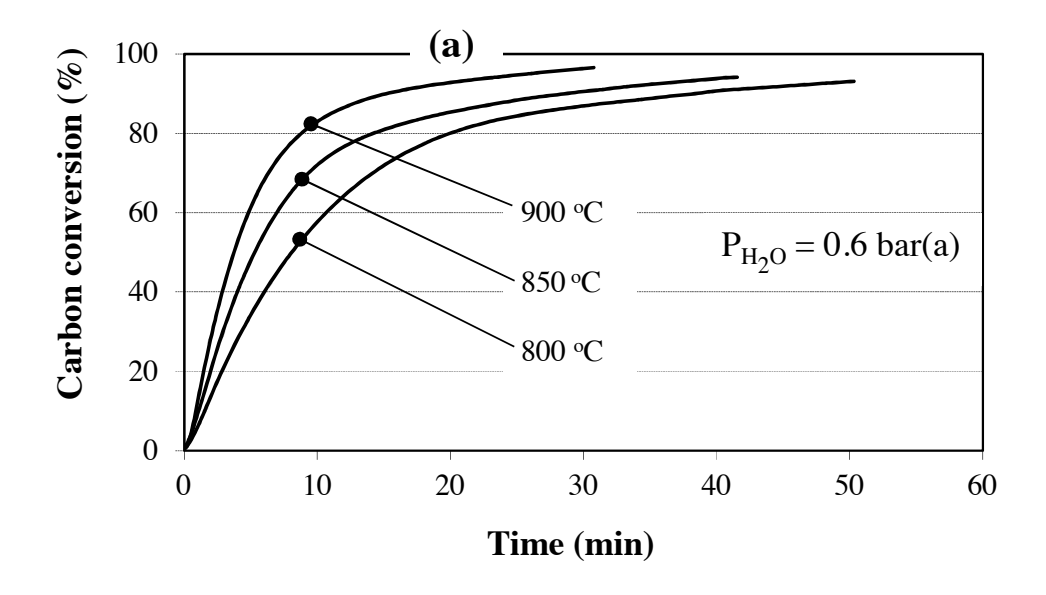


Figure 2



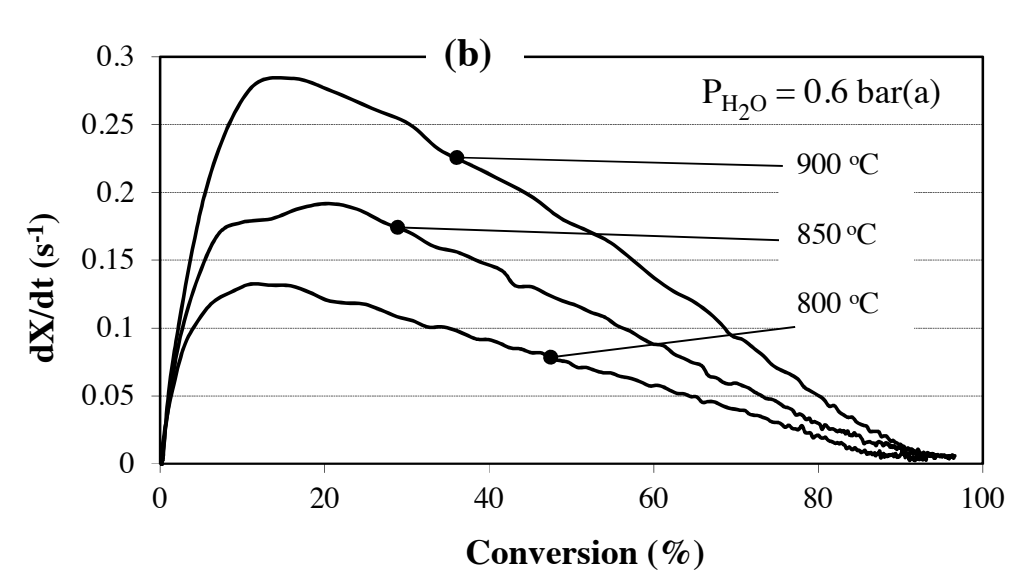
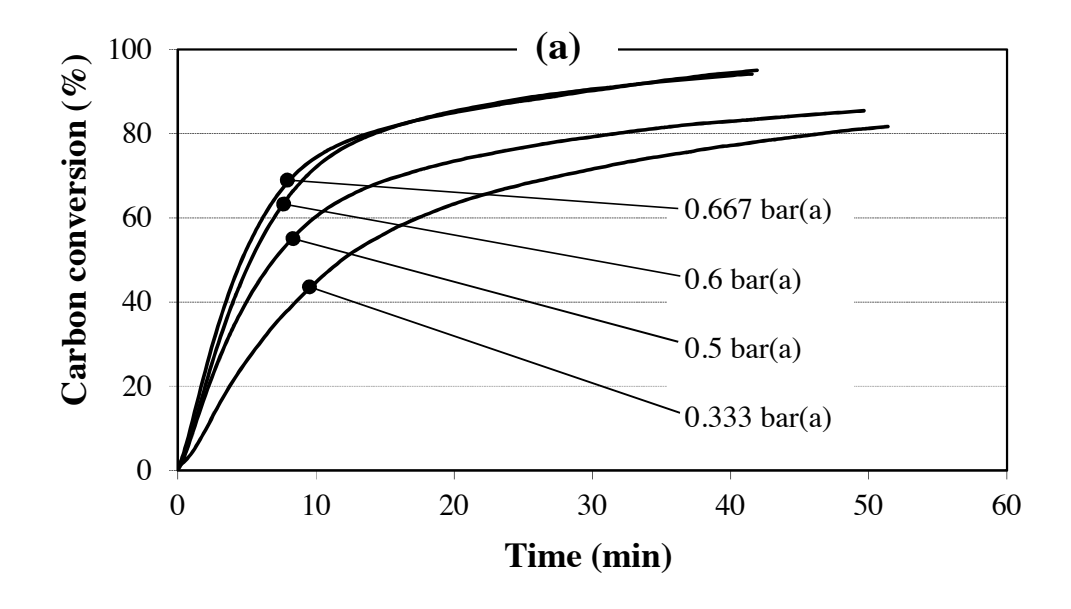


Figure 3



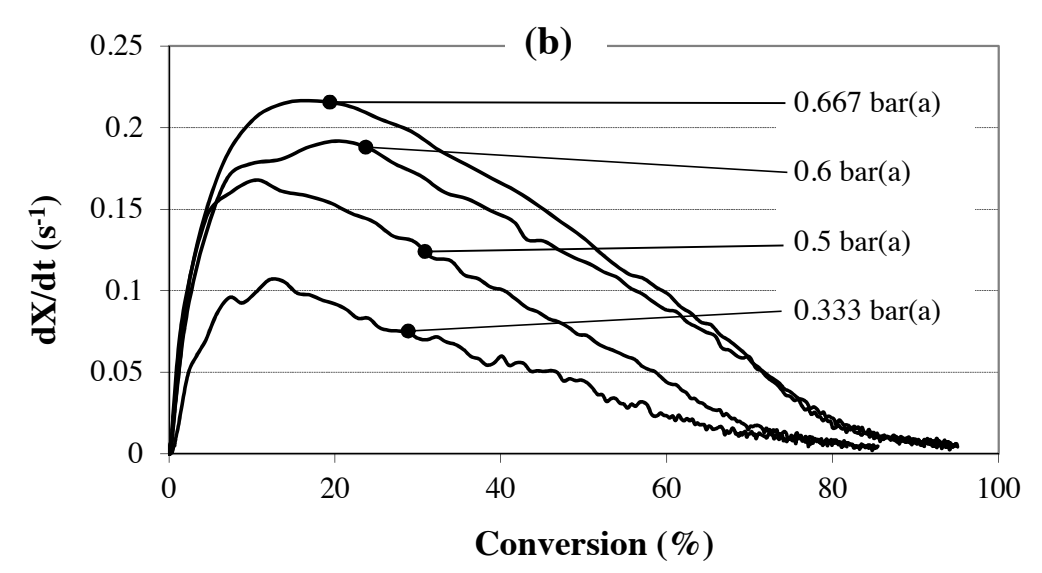


Figure 4

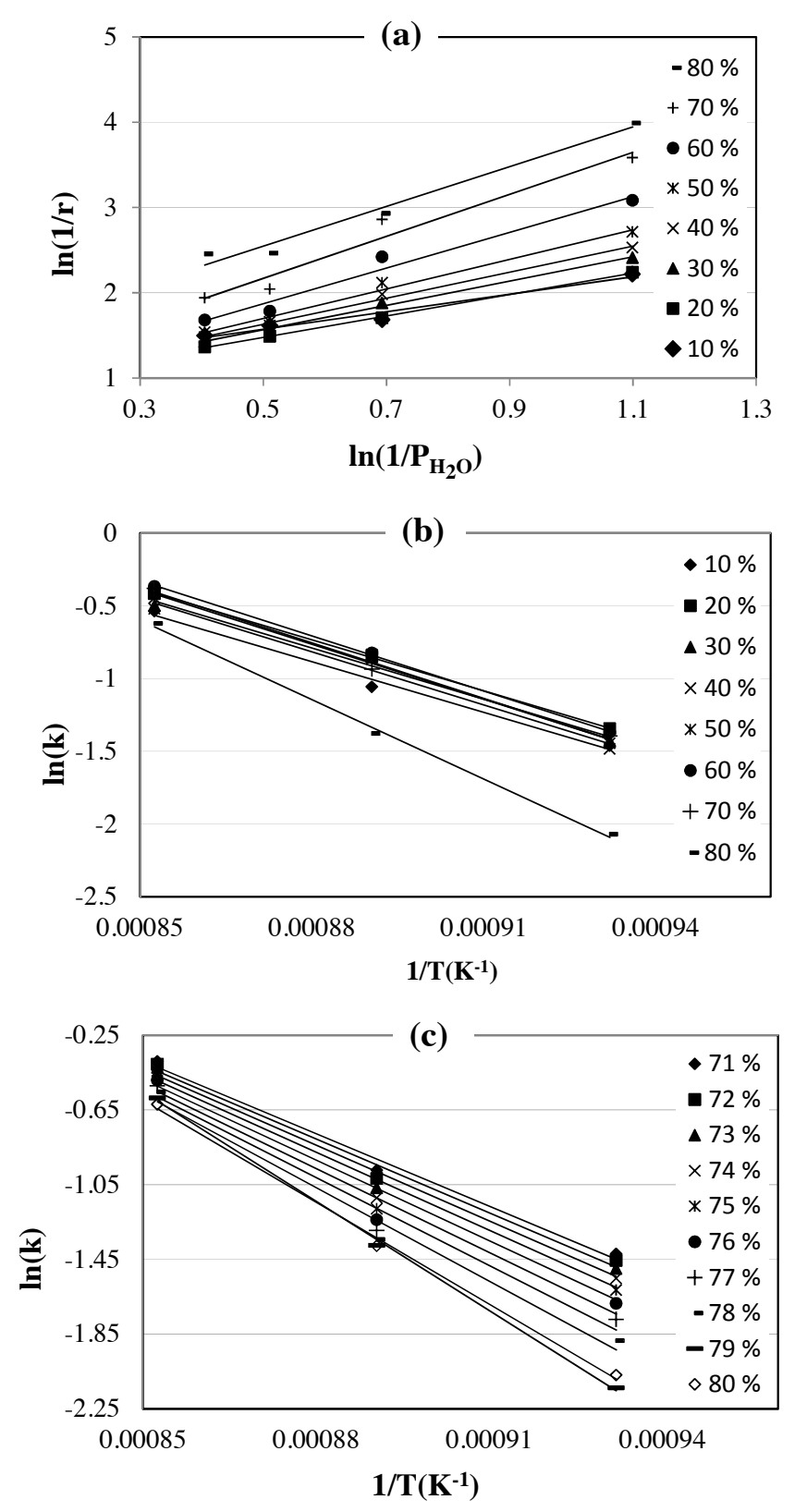


Figure 5

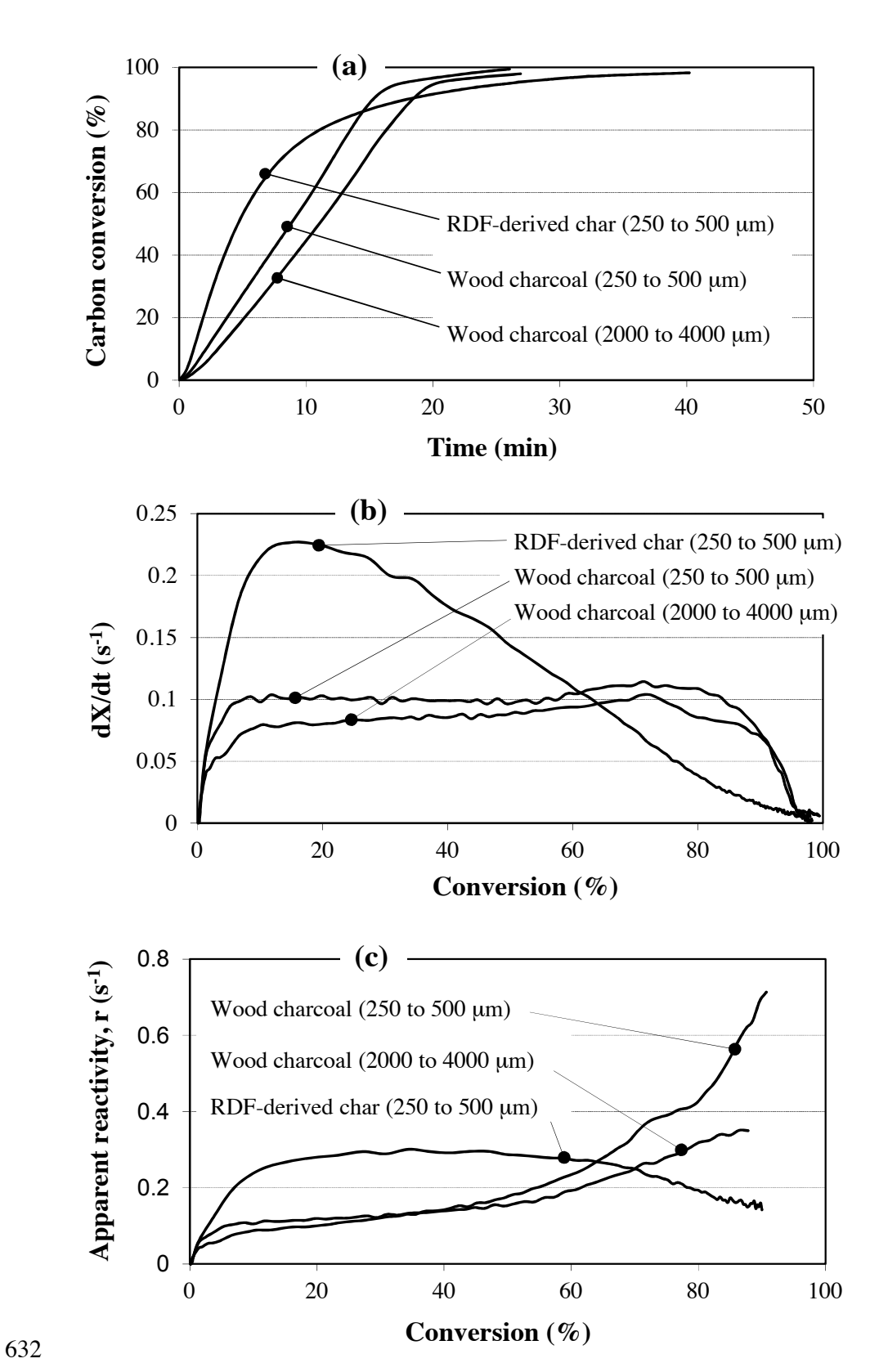


Figure 6

Table 1. Values of k and n at various reaction temperatures (Shrinking-Core Model).

Carbon	900) °C	850) °C	800	O°C
conversion (%)	k	n	k	n	k	n
10	0.585	1.453	0.347	1.025	0.232	0.889
20	0.660	1.413	0.429	1.261	0.261	1.075
30	0.607	1.370	0.427	1.429	0.239	1.179
40	0.594	1.409	0.421	1.529	0.226	1.216
50	0.639	1.579	0.435	1.732	0.235	1.382
60	0.693	1.878	0.439	2.092	0.254	1.810
70	0.684	2.286	0.393	2.466	0.248	2.351
80	0.537	2.676	0.252	2.333	0.126	2.937

Table 2. Apparent activation energies and pre-exponential factors (Shrinking-CoreModel).

Carbon	Arrhenius equation	Apparent	Pre-exponential
conversion (%)	$\ln(k) = \ln(A) - \frac{E}{R_o} \frac{1}{T}$	activation energy,	factor, A (bar- $^{-n}$ s- $^{-1}$)
	$R_g T$	E (kJ mol ⁻¹)	
10	y=9.342 - 11620x	96.6	1.14 x 10 ⁴
20	y=9.5596 – 11696x	97.2	1.42×10^4
30	y= 9.5651 – 11768x	97.8	1.43×10^4
40	y = 9.9045 - 12182x	101	2.00×10^4
50	y=10.323 - 12597x	105	3.04×10^4
60	y=10.42 - 12644x	105	3.35×10^4
70	y=10.471 – 12756x	106	3.53×10^4
71	y=10.612 - 12942x	108	4.06×10^4
72	y=10.806-13195x	110	4.93×10^4
73	y= 11.061 – 13522x	112	6.36×10^4
74	y= 11.379 – 13926x	116	8.75×10^4
75	y= 11.765 – 14412x	120	12.9×10^4
76	y=12.225 - 14987x	125	20.4×10^4
77	y=12.798 - 15695x	131	36.1×10^4
78	y= 13.651 – 16724x	139	84.8×10^4
79	y= 16.035 – 19516x	162	92.0×10^5
80	y= 14.889 – 18220x	152	29.3 x 10 ⁵

Note: When the conversion was calculated, using the equations presented in this table,

the match was within \pm 5% of the experimental data obtained.

Table 3. Apparent activation energies and pre-exponential factors (Uniform-Reaction Model).

conversion (%)	E = 1	4:4:	
	$\ln(K) = \ln(A) - \dots - \dots$	activation energy,	factor, A (bar-n s-1)
	$\ln(k) = \ln(A) - \frac{E}{R_g} \frac{1}{T}$	E (kJ mol ⁻¹)	
10	y=9.3771 – 11620x	96.6	1.18 x 10 ⁴
20	y=9.6351 – 11697x	97.2	1.53×10^4
30	y = 9.684 - 11768x	97.8	1.61×10^4
40	y= 10.075 - 12182x	101	2.37×10^4
50	y=10.555-12598x	105	3.84×10^4
60	y=10.725 - 12644x	105	4.55×10^4
70	y=10.873 - 12756x	106	5.27×10^4
71	y=11.023 - 12941x	108	6.13×10^4
72	y=11.231 – 13195x	110	7.54×10^4
73	y= 11.498 – 13522x	112	9.85×10^4
74	y= 11.828 – 13926x	116	13.7×10^4
75	y= 12.227 - 14412x	120	20.4×10^4
76	y=12.7 - 14987x	125	32.8×10^4
77	y=13.228 - 15695x	131	59.0 x 10 ⁴
78	y= 14.155 – 16723x	139	14.0 x 10 ⁵
79	y= 16.525 – 19482x	162	15.0×10^6
80	y=15.426 - 18220x	152	50.1 x 10 ⁵

Note: When the conversion was calculated, using the equations presented in this table,

the match was within \pm 5% of the experimental data obtained.